



LJMU Research Online

Al-Baghdadi, HM, Kadhum, MM and Shubbar, A

Evaluate the bonding strength performance between lightweight concrete and lightweight engineered cementitious composite using different percentages of cenosphere and hybrid fibers

<https://researchonline.ljmu.ac.uk/id/eprint/26634/>

Article

Citation (please note it is advisable to refer to the publisher's version if you intend to cite from this work)

Al-Baghdadi, HM, Kadhum, MM and Shubbar, A (2025) Evaluate the bonding strength performance between lightweight concrete and lightweight engineered cementitious composite using different percentages of cenosphere and hybrid fibers. Journal of Building Pathology and

LJMU has developed **LJMU Research Online** for users to access the research output of the University more effectively. Copyright © and Moral Rights for the papers on this site are retained by the individual authors and/or other copyright owners. Users may download and/or print one copy of any article(s) in LJMU Research Online to facilitate their private study or for non-commercial research. You may not engage in further distribution of the material or use it for any profit-making activities or any commercial gain.

The version presented here may differ from the published version or from the version of the record. Please see the repository URL above for details on accessing the published version and note that access may require a subscription.

For more information please contact researchonline@ljmu.ac.uk

<http://researchonline.ljmu.ac.uk/>



Evaluate the bonding strength performance between lightweight concrete and lightweight engineered cementitious composite using different percentages of cenosphere and hybrid fibers

Haider M. Al-Baghdadi¹ · Mohammed M. Kadhum¹ · Ali Shubbar²

Received: 14 February 2025 / Revised: 27 May 2025 / Accepted: 3 June 2025
© The Author(s) 2025

Abstract

The objective of this research is to investigate the bond performance of high-strength lightweight concrete (HLWC) substrate and lightweight engineered cementitious composites (LECC) used as overlay repair materials with varying amounts (0%, 30%, 70%, and 90%) of fly ash cenosphere (FAC) as a replacement of sand with different surface roughness conditions (as-cast surface and grooved surface). In the preparation of the LECC mixtures, a novel combination of polyvinyl alcohol (PVA) and glass fibers (GF) was used. Mechanical properties such as compressive strength, flexural strength, and density of the HLWC and LECC were tested. Additionally, the bond strength at the interface between the HLWC substrate and the LECC was evaluated by conducting both the slant shear test and the direct shear test (bi-surface) at the age of 28 days. Results indicated that replacing the sand with 70% FAC reduced the density of the LECC by about 35% and improved the specific strength ratio by about 8.6% relative to the mixture with 0% FAC. Results also showed that for both tests (slant shear and bi-surface shear), maximum bond strength was recorded for the grooved surface. For the grooved surface under the slant shear test, replacing the sand with 30% and 70% FAC provided a bond strength of 21.85 MPa and 18.35 MPa, respectively. For bi-surface shear, replacing the sand with 30% and 70% FAC showed a bond strength of 13.85 MPa and 10.3 MPa, respectively. This research reported on the production of a repair material with comparable strength, a high specific strength ratio, and an outstanding strength-to-weight reduction ratio, making it the perfect option for repair applications where durability and load-bearing capability are essential.

Keywords Lightweight engineered cementitious composite · Fly ash cenosphere · Bi-surface shear test · Grooved surface · Slant shear test

1 Introduction

Deterioration of existing concrete structures is common due to aging, overloading, accidental damage, and exposure to fire. In recent years, repairing such structures has

become more attractive than demolition and reconstruction for several reasons such as cost, reducing the consumption of natural resources, and conserving virgin lands from being landfills for demolition waste [11]. The bond strength in the interface zone between two concretes plays a crucial role in ensuring the uniform performance of both materials. The bond strength depends mainly on two factors, (1) the roughness and interlocking of the bonding area and (2) the chemical reaction between the substrata and the overlay material.

Engineered Cementitious Composites (ECC) is a type of cement-fly ash-based composite that is reinforced with fibers [36]. ECC is known for its exceptional tensile strain capacity and high ductility, achieved by including a moderate amount of fibers (usually 2% by volume) [35]. Additionally, ECC exhibits excellent compressive strength, often ranging from 40 to 120 Mpa [44]. Due to such desirable properties, ECC has been used as repair materials [18, 49].

✉ Ali Shubbar
A.A.Shubbar@ljmu.ac.uk

Haider M. Al-Baghdadi
eng.haider.m@uobabylon.edu.iq

Mohammed M. Kadhum
eng.mohammed.mansour@uobabylon.edu.iq

¹ Civil Engineering Department, College of Engineering, University of Babylon, Babylon, Iraq

² School of Civil Engineering and Built Environment, Liverpool John Moores University, Liverpool L3 3AF, UK

Researchers have studied the use of ECC strengthening in reinforced concrete structures such as beams, columns, and beam-column junctions [34, 37]. When ECC is added to a structural element, many tiny cracks develop on the surfaces experiencing tension or complicated stress, such as the beam's underside and the joint's core region. Despite this, the structural element's load-bearing capability remains unaffected. This process of successive cracking typically leads to a ductile failure mode. The results indicated that the binding strengths between ECC and concrete, such as interfacial tensile strength and interfacial shear strength, are sufficient to transmit force from the original RC structure to the strengthening layer. The binding strength is positively correlated with the surface roughness.

An essential component of the ECC is the usage of up to 2% (by volume) of fiber to enhance the tensile strain capacity. Different types of fibers were used in the development of ECC such as polyvinyl alcohol (PVA) fibers [19, 20], Jiangtao [45], polypropylene (PP) [49], glass fibers (GF) [31] and combination of these types of fibers [13]. A recent study that was conducted by the authors of this paper [3] to find the best combination of PVA fiber and GF found that the a combination of 1.5% PVA + 0.5% GF provided the best performance. Therefore, in this research, this hybrid combination of fibers was employed.

The density of ordinary-weight ECC is approximately 2100 kg/m³. The construction of lightweight ECC (LECC) has gained scientific attention due to inherited high ductility and lower unit weight [11, 23, 25]. To produce LECC, various lightweight aggregates/fillers, such as expanded glass, glass cenospheres, fly ash cenospheres (FAC), and pumice, can be used. Hanif et al. [20] investigated the suitability of using glass cenospheres to replace up to 50% of cement in the production of LECC. Results indicated that replacing cement with 30% glass cenospheres resulted in a density of about 1162 kg/m³ and corresponding compressive strength of 33 Mpa. Additionally, FAC was employed by [19, 20] to replace cement in the range of 30–70% to develop LECC. They found that the density was ranging between 1260 and 1612 kg/m³ and the compressive strength was ranging between 30.38 Mpa and 55.92 Mpa. Moreover, Zhou et al. [49], examined the suitability of FAC as sand replacement material in the range of 20–60% in the production of LECC. Results showed that by increasing the FAC content, the density was reduced and reached its minimum value of 1380 kg/m³ for the mixture with 60% FCA. According to the above studies, FAC shows promise for recycling into cementitious materials that can be used to create lightweight ECC [30]. FAC, together with fly ash, are significant byproducts of coal power stations. FAC are hollow particles that develop when glass cools rapidly after coal combustion for power production [47].

Extensive research has focused on investigating the bond between substrate and overlay concretes [11, 32, 38], B. [40, 50]. These investigations have mostly been conducted on composite specimens of a substrate (regular concrete) and an overlay material. Limited studies investigated the bond performance between high-strength lightweight concrete and lightweight ECC made with high volume fraction (up to 90% FAC) as sand replacement material and included a hybrid combination of (1.5% PVA + 0.5% GF) fibers [3]. Therefore, this study will investigate the bond behavior at the interface between hybrid fiber-reinforced (1.5% PVA + 0.5% GF) lightweight ECC containing a high-volume fraction of FAC and high-strength lightweight concrete surfaces with different surface preparation.

2 Materials and methods

Each analyzed sample consists of two different types of concrete, namely the substrate concrete (high strength lightweight concrete (HLWC)) and the overlay material, Lightweight Engineered Cementitious Composite (LECC), with different proportions of FAC, replacing sand at percentages of 0%, 30%, 70%, and 90% and hybrid fibers (1.5% (Polyvinyl alcohol) PVA + 0.5% Glass fibers (GF)). Many factors were considered, including the test method, proportions of FAC, and the roughness of the substrate at 28 days' age of the composite samples.

2.1 Materials

Cement: for all mixtures, Ordinary Portland cement from MASS Iraq Company was used. The cement undergoes testing to verify its compliance with Iraqi Standard No. 5/1984 (Iraqi Standards NO.5 1984) and BS EN 197–1 [15].

Sand: natural sand from AL-Ekhaider region was used in this research. Table 1 presents the sieve analysis results conducted on the natural sand. The natural sand was spread out and allowed to dry in the open air. Additionally, the chemical and physical characteristics were examined. The findings indicate that the natural sand grading complied with the Iraqi Specification No. 45/1984, (Iraqi Standards NO.45 1984), and ASTM C128, [6].

Coarse aggregate: this research used lightweight expanded clay aggregate (LECA) (Fig. 1). LECA is made from porous ceramic materials with uniformly small closed-cell pores as well as firmly sintered and durable exterior surfaces. Table 2 presents the sieve analysis of LECA that follows the ASTM C330-17a [8] Limits. Additionally, Table 3 displays the physical and chemical characteristics of LECA. As advised by ACI 211.2–98 (ACI 211.2–98 2004), LECA soaked in water for at least 48 h due to its high water absorption capacity to prevent it from absorbing water during

Table 1 Physical and chemical properties and the grading of the used sand

Size of sieve mm	% Cumulative passing	Limits of IQS No. 45/1984 as in (Zone 2)	Physical properties	Test results
10	100	100	Specific gravity	2.62
4.75	90	90–100	Absorption	0.91%
2.36	88	75–100	Fine material passing from the sieve (75 μm)	2.3%
1.18	72	55–90	Fineness modulus	2.67
0.60	55	35–59		
0.30	23	8–30	Chemical properties	
0.15	5	0–10	Sulfate content	0.21%

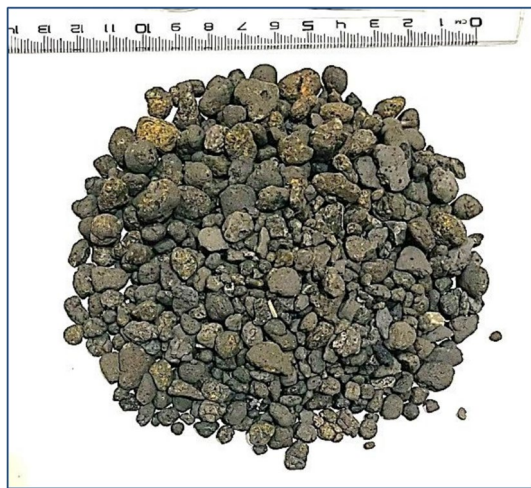


Fig. 1 lightweight expanded clay aggregate (LECA)

Table 2 Grading of used LECA coarse aggregate

Size of sieve (mm)	Cumulative passing %	Limits of ASTM C330-17a, 2017
	Structural LECA	
12.5	100	100
10	99	80–100
8	66	–
6	44	–
4.75	7	5–40
2.36	2	0–20
1.18	0	0–10

mixing. After that, it was distributed in laboratory air until the surface dried, leaving the aggregate in a saturated and surface-dry state (SSD).

Silica fume: in this research, silica fume, which is available commercially under the name MasterRoc®MS 610 OR BASF silica fume from Master Builders Solutions, was used to replace cement partially by 15%. The used Silica fume

Table 3 Physical and chemical properties of LECA

Chemical properties		Physical properties	
Chemical composition	Percentage by weight%	Properties	Test results
CaO	3.78	Specific Gravity	1.2
SiO ₂	61.58	Water Absorption	12%
Al ₂ O ₃	16.99	Bulk density kg/m ³	700
Fe ₂ O ₃	7.62		
MgO	2.56		
SO ₃	0.19		
Na ₂ O	1.03		
Loss on Ignition	0.2		

Table 4 Properties of the superplasticizer (Master Glenium 54)

Color	Whitish to straw
Specific gravity	1.07
PH	5–7
Chloride content	None
Toxicity	Danger hazardous material
Fire	Not fire-propagating

density of 0.55–0.7 kg/L, and chloride concentration of less than 0.1% [24].

High-range water reducer (HRWR): High-performance concrete superplasticizer Master Glenium 54 was used in this research. A percentage of 3.7% was added to the mixtures to generate a workable flow for ECC. Table 4 displays the properties of the Master Glenium 54.

PVA fiber: Polyvinyl Alcohol (PVA) was used in this research. Figure 2 shows the used PVA fiber and Table 5 presents the properties of the PVA fiber.

Glass fiber (GF): a different kind of fiber, was added to ECC with PVA fiber in this research. Figure 3 shows the used GF and Table 5 presents the properties of the GF.

Fly Ash: Fly ash has been a common ingredient in structural concrete, which normally has an ash percentage of

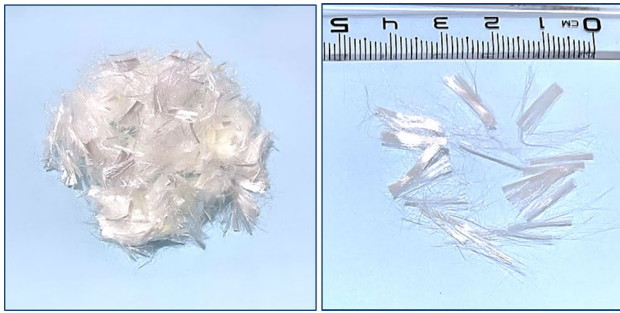


Fig. 2 Polyvinyl Alcohol fiber geometry

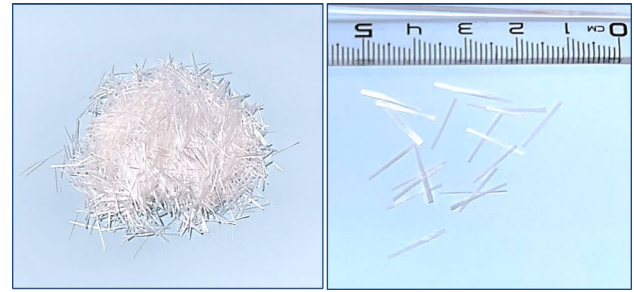


Fig. 3 Glass fiber geometry

10–30% (Pradhan, and Panda, 2017). However, in ECC mixes, Fly ash content ranges from 120 to 220% [39]. The fly ash used in this research was provided by Eurobuild Flyash and it complies with BS EN 450 [14]. The used Fly ash was class F. It had a Blaine-specific surface area of 2970 cm²/g and a specific gravity of 2.70 g/cm³. Table 6 lists the chemical properties of fly ash.

Fly ash cenospheres (FAC): In this work, fly ash cenospheres (FAC) having a bulk density of around 400 kg/m³ were utilized as lightweight fine aggregates to replace sand in proportions of 0%, 30%, 70%, and 90% by weight. The range of the FACs’ particle size was 45 μm to 300 μm. Table 7 lists the chemical components of the FAC. FAC particles have a low apparent density and good thermal insulation because of their thin shell and hollow microstructure. Table 8 presents the physical properties of FAC. The FAC utilized in this study is shown in Fig. 4.

2.2 High-strength lightweight concrete (HLWC) substrate and lightweight engineered cementitious composites (LECC) overlay mix properties

2.2.1 LWC substrate mixes properties

The mix design of the HLWC has been designed to attain a compressive strength results of 50 Mpa at the age of 28 days according to the ACI Committee 211.2–98 (ACI 211.2–98 [1]) and ACI 211.4R-08 (ACI. 211.4R-08 [2]) guidelines. Table 9 shows the mixture ratio and mix details for HLWC. This mix design was selected following range of trial mixes to achieve both the required strength and proper workability.

Table 5 Properties of PVA and GF

Fiber	Fiber length (mm)	Diameter (μm)	Tensile strength (Mpa)	Young’s modulus (Gpa)	Fiber Elongation (%)	Density (kg/m ³)
PVA	12	39	1600	40	4–10	1.3
GF	12	–	2200	80	0–4	2.78

Table 6 Chemical properties of Fly Ash (Type F) used

Chemical composition	% by weight
Al ₂ O ₃	24.62
SiO ₂	48.53
CaO	9.49
Fe ₂ O ₃	7.59
K ₂ O	2.51
MgO	2.28
Na ₂ O	1.18
SO ₃	2.48
Loss on ignition	1.69
Activity	
28 d activity index	90%

2.2.2 LECC overlays mix properties.

Table 10 presents the mix design of the ECC. The entire amount of cementitious material, or cement and fly ash (Type F) in ECC, is known as the binder system. In this research, the standard fly ash-to-cement ratio of 1.2 was used [39],S. [42],Jing [46]. For proper stiffness and volume stability, ECC uses fine silica sand with a sand-to-binder ratio (S/B) of 0.36. To achieve a suitable combination of fresh and hardened qualities, ECC has a water-to-binder (w/b) ratio of 0.26 and an HRWR of 0.012. Many trial mixes have been prepared to achieve the optimum dosage of HRWR to get fresh properties for ECC mortars with a mini-slump flow range between (240–260) mm, while at the same time achieving an easy to mixing with fiber (PVA and Glass fiber) without the wrapping and twisting of the

Table 7 Chemical composition of FAC

SiO ₂	Al ₂ O ₃	Fe ₂ O ₃	MgO	CaO	K ₂ O	SO ₃	Na ₂ O
69.4	23.12	3.10	0.80	1.04	0.30	1.20	0.02

Table 8 Physical characteristics of FAC

Apparent density (g/cm ³)	Bulk density (g/cm ³)	Crushing strength (Mpa)	Moisture %	Melting point °C	Thermal conductivity W/mK	Moisture content (%)
0.78	0.44	70	0.10	1600	0.08	0.20

**Fig. 4** Fly ash cenospheres (FAC)

fibers, which restricts the operation of mixing and pouring, and complete penetration of prepared mortars through the reinforcement and concrete mold specified for repair. The dosage of hybrid fibers volumes of (PVA 1.5% + GF 0.5%) that has been used in this research are based on a recent study that was conducted by the authors of this paper [3] to find the best combination of PVA fiber and GF.

Four mixes of LECC, substituting different proportions of FAC for sand, 0%, 30%, 70%, and 90% were used as overlay materials as shown in Table 11.

Table 9 Mix proportions of HLWC (kg/m³)

Nomenclature	Cement kg/m ³	Sand kg/m ³	LECA g/m ³	Silica fume kg/m ³	Water kg/m ³	HRWR by wt. of cm (%)	W/C
HLWC	550	678	400	81	160	1.7	0.25

Table 10 ECC Mix Design Proportions by Weight for ECC

Mix Design	Cement	Fly ash	Sand	Water	HRWR	Hybrid fiber Vol. %
1	1	1.2	0.8	0.56	0.012	PVA 1.5% + GF 0.5%

2.3 Preparation of composite specimens (HLWC-LECC)

Composite specimens with varying HLWC substrates and LECC overlay materials were created and tested in succession. The interface bond strength at age 28 days was assessed using both the slant shear test and the bi-surface shear test. The samples used in this research were 75 × 150 mm cylinders with a 30° inclination angle (α) measured about the vertical axis (ASTM C882/C882M 2020). The remaining test specimens were 150 mm cubes, of which one-third contained the overlay material (LECC) and the other two-thirds were the HLWC substrate (Ayat [27]). To create an HLWC substrate in these styles, wood cubes with a height of 150 mm and a base size of 50 × 150 mm were cut, as indicated in Fig. 5 and Fig. 6. Wood cylinders were cut in the slanted dimension of the cylinder shape and the designated direction. Primarily, the casted HLWC substrate filled half the cylindrical molds and two-thirds of the cubic molds. The newly mixed HLWC substrate mixes remained in the molds for a day. Subsequently, the specimens underwent a 28-day immersion in water. The HLWC substrate samples undergo two types of surface preparation procedures: grooved (grooves inclined at about a 45-degree angle) and as-casting.

It is necessary to moisten the HLWC-substrate interface to attain saturated surface dry (SSD) conditions before applying the overlay, as stated by Beushausen et al. [12]. Wetting the HLWC substrate overlay interfaces, followed by wiping with a damp cloth. To finish these cylinders, SSD slanted cutting specimens were put into cylinder molds with

Table 11 LECC mixtures with different cenosphere content

Nomenclature	LECC uses different percentages of FAC in replacement of sand	Number of samples tested		
		Compressive strength	Flexural strength	Density
0%	LECC0	3	3	3
30%	LECC30	3	3	3
70%	LECC70	3	3	3
90%	LECC90	3	3	3

the bevel side facing up. The employed overlay materials were then poured on top of the HLWC substrate concrete. In contrast, SSD bi-surface cutting specimens were put into cube molds, and to finish the cubes, an overlay material made up of one-third of the cubes was applied.

2.4 Surface preparation

Many investigations have determined that the degree of roughness of the substrate surfaces has a significant impact on the bond strength between two materials [12, 17, 28].

High accuracy was considered in the implementation of this stage as a rough surface that ensures a relatively perfect bond between the concrete substrate body and the repairing material is required to ensure that the LECC repair material contributes to bearing part of the stresses. In this study, the grooving method and as-cast surface method were used to obtain quantitative surface roughness parameters for the lightweight concrete surfaces of the specimens. To guarantee an excellent interlock between the concrete surface and the LECC layer, grooves were cut at an angle of 45 degrees using specialized stone-cutting

discs to provide a precise binding. The applied grooves were 2 mm wide and had a depth of 2.5 mm and the distance between these grooves was 18–20 mm (Fig. 7). Following the roughing procedure, a water extrusion and compressed air cleaning were used to make sure there was no dust left. The specimens were then allowed to dry before the LECC repair material was applied.

2.5 Test setup

The most common test procedures for estimating the bond strength at the interface between concrete substrate and overlay repair material are Pull-off, pull-off, splitting prism, slant shear, and Bi-Surface shear methods [16], A [26]. According to A Momayez et al. [26] slant shear and Bi-Surface shear test methods can predict values of the bond strength of composite materials that are about 80% of the bond strength of samples cast monolithically. Therefore, both tests were considered in this research to evaluate the performance of the bond strength of composite materials under various parameters.

2.5.1 Slant shear test

The slant shear test was conducted according to ASTM C882/C882M (ASTM C882/C882M [10]). The slant shear test is considered one of the most reliable methods that provide consistent results of bond strength [11, 25]. As can be seen in Fig. 8a, specimens were evaluated using a standard compression device. The application of the loading followed the ASTM C39/C39M (ASTM C39/C39M [10]) recommendations. Recording the maximum load values allowed

Fig. 5 Wood slices for **a**-slant shear, **b**-bi-surface shear test

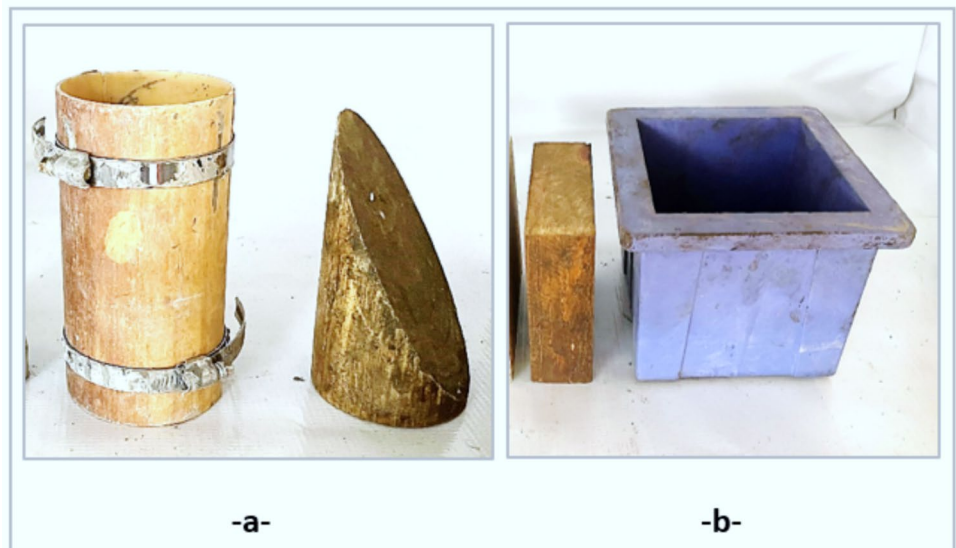


Fig. 6 Preparation of composite specimens **a**-slant shear, **b**- bi-surface shear

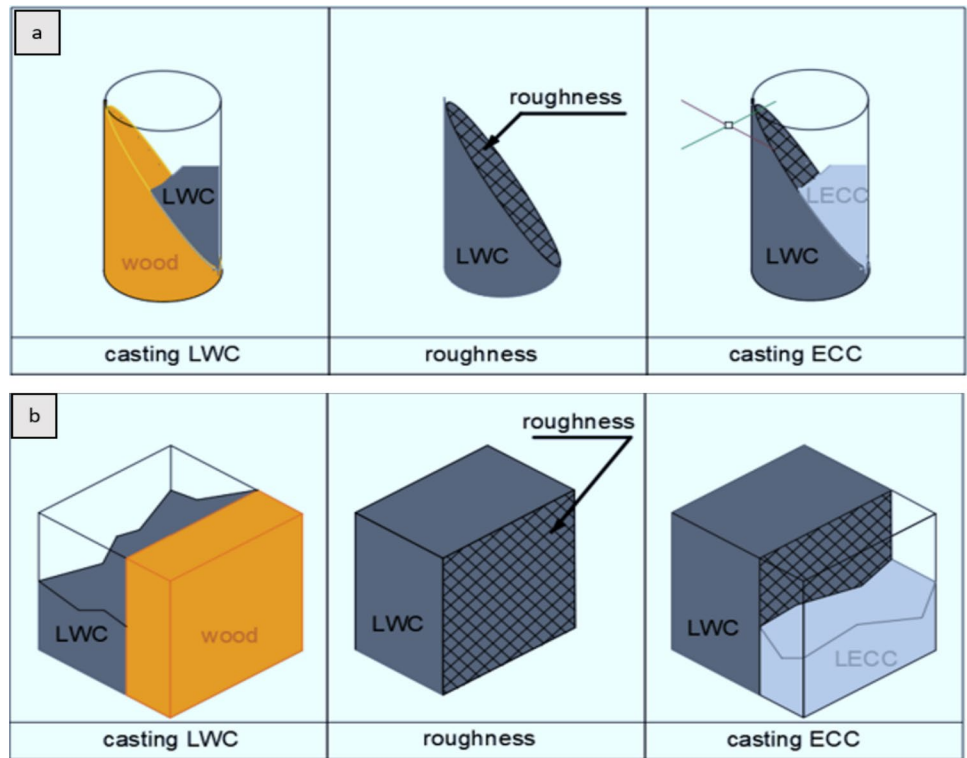


Fig. 7 Roughing process **a**- half cylinder grooved and as cast surface **b**- Two-thirds of the cube grooved and as cast surface



Eq. (1) to calculate the applied stress σ_o (Mpa) needed to cause bond rupture.

$$\sigma_o = P/Ae \tag{1}$$

P is the maximum applied load (in Newtons) and Ae is the slant surface’s elliptical area (in mm²). Equations (2) and (3), which describe the shear and compressive strengths of the bond in Fig. 8(b), together determine the maximum applied stress.

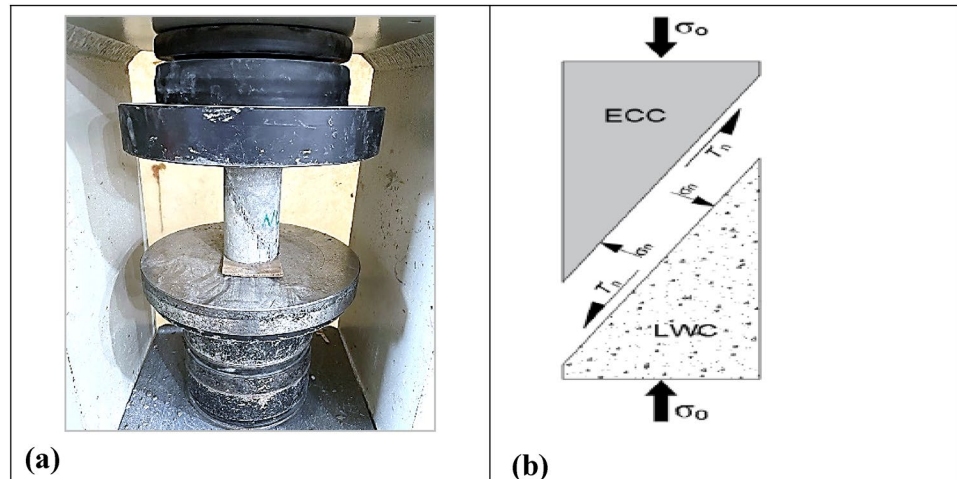
$$\tau_n = \sigma_o \cos \alpha \tag{2}$$

$$\sigma_n = \sigma_o \sin 2\alpha \tag{3}$$

In Eqns. (2) and (3), $\alpha = 30^\circ$ while τ_n and σ_n are shear and compressive stresses acting on the bond plane, respectively. τ_n and σ_n are related in the form as in Eq. 4 [48].

$$\tau_n = c + \mu \sigma_n = c + \tan \phi \cdot \sigma_n \tag{4}$$

Fig. 8 Slant shear test **a-** compression test, **b-** Stresses developed at the interface



where c , μ , and ϕ are cohesion, coefficient of friction, and internal angle of friction of the bond, respectively. For each mixture three specimens were prepared and tested for Slant shear.

2.5.2 Bi-surface shear test

Momayez et al. (A [26]) suggested a Bi-surface shear test technique to ascertain the average shear bond strength between two kinds of concrete. This study followed the suggested approach as this test yields reliable findings and is simple to administer. For each mixture three specimens were prepared and tested for Bi-surface shear. All specimens were subjected to a continuous loading rate of 2 kN/s using a 2000 kN digital testing apparatus. Equation (5) was utilized to ascertain the values of the bi-surface shear strength. To determine the direct shear strength, the mean of the two shear force values was considered. Figure 9 displays the testing apparatus and configuration.

$$\tau_v = P_v / (2 \times A_v) \quad (5)$$

where: τ_v = Bi-surface shear bond strength (Mpa), P_v = Ultimate load indicated by the testing machine (N), A_v = Area of interface in shear (mm^2).

2.5.3 Compressive strength and flexural test

The compressive strength test of the HLWC was conducted using three cubes of 150 mm \times 150 mm \times 150 mm according to the ASTM C39/C39M (ASTM C39/C39M [10]). To find the compressive strength of LECC, three cube specimens measuring 70 mm \times 70 mm \times 70 mm were made.



Fig. 9 Bi-surface shear test

The compressive strength test was conducted according to the ASTM C109 (ASTM C109/C109M-13e1 [5]). For each mixture three specimens were prepared and tested for compressive strength.

The flexural strength of both the HLWC and the LECC was conducted using four prisms with dimensions of 100 mm \times 100 mm \times 40 mm according to ASTM C293/C293M (ASTM C293/C293M [7]) for each mixture. For each mixture three specimens were prepared and tested for flexural strength.

2.5.4 Density test

The apparent density test was conducted according to ASTM C642 (ASTM C642-21 [10]). To ascertain the density of LECC, the 50 mm cubes were used. Firstly, the samples were dried at 105 °C in an oven. The specimens were then

allowed to cool in the air. After that, the specimen is suspended by a wire in water, and the apparent mass immersed is calculated. For each mixture three specimens were prepared and tested for density.

It is possible to calculate the apparent density using Eq. (6):

$$\rho A = [A/(A - D)] \cdot \rho_w \quad (6)$$

where:

- ρA is the apparent density of the sample (in g/cm^3);
- ρ_w is the density of water (in g/cm^3);
- A is the mass of the oven-dried sample in air (in g); and.
- D is the apparent mass of the oven-dried sample in water (in g).

3 Results and discussion

3.1 Mechanical properties

The mechanical properties of the HLWC (Compressive and flexural strength) and density were tested at 28 days (Table 12). The same tests were performed on the LECC mixtures with different FAC content, and the results are summarized in Table 13. From Table 12 and Table 13, the compressive strength of the LECC samples made with up to 70% FAC was higher than that of the HLWC. This performance could be mainly attributed to the pozzolanic reaction of the Fly ash and FAC which generates secondary hydrated calcium silicate gel (C–S–H) that in turn produces a denser structure and thus improves the compressive strength [11],

[41]. On the other hand, the lower compressive strength of the mixture with 90% FAC (LECC90) relative to the HLWC could be attributed to its lower density in comparison with the density of the HLWC. Regarding the flexural strength, it can be seen from Tables 12 and 13 that all the LECC mixtures have shown higher flexural strength relative to the HLWC. This is mainly attributed to the presence of fibers in the LECC [29]. According to Table 13, replacing the sand with up to 70% FAC resulted in higher specific strength % (compressive strength/ density) relative to the ECC mixture with 0% FAC (LECC0). Considering both strength and density, it can be stated that the positive impact of using FAC in ECC is developing a higher specific strength and reducing the overall weight of ECC making it a perfect option for repair applications where durability and load-bearing capability are essential. [43]. In a comparison with the findings of [49], comparable density and compressive strength were recorded for the mixture with 30% FAC. Additionally, in this research higher replacement levels (70% FAC) have shown higher compressive strength (59 MPa) in cooperation with their mixture that contain 60% FAC that showed about 42 MPa.

Figure 10 shows the density compressive strength of LECC mixtures. As can be seen in Fig. 10, the density of the mixtures decreased with increasing the FAC content. For the mixture with 90% FAC (LECC90), the density was reduced by about 41% relative to the control mixture (LECC0). On the other hand, increasing the FAC content resulted in a significant reduction in the compressive strength reaching about 48% for the LECC90 relative to LECC0. The reduction in the compressive and flexural strength of LECC with increasing the FAC content could be attributed to the lightweight and hollow nature of the FAC that contributed to the decrease in the density and strength of the LECC [33, 49]. Figure 11 presents the specific strength (strength per unit density) results of the mixtures. The specific strength of LECC30 and LECC70 were higher than the control mixture (LECC0). The improved specific strength of LECC is attributed to the incorporation of lightweight FAC. On the other hand, the lower specific strength of the LECC90 relative to the control mixture could be attributed to its low compressive strength.

Table 12 Mechanical Properties of HLWC

Mechanical property	Unite	HLWC	Number of samples tested
Compressive Strength	Mpa	54.25	3
Flexural Strength	Mpa	6.80	3
Density	(kg/m^3)	1605	3

Table 13 Mechanical Properties of LECC

Nomenclature	% of FAC as replacement of sand	Density kg/m^3	Average of compressive strength at 28 days (Mpa)	Flexural strength at 28 days (Mpa)	specific strength % (compressive strength/ Density)
LECC0	0%	2180	84	21.50	3.85
LECC30	30%	1780	70	19.60	3.93
LECC70	70%	1410	59	16.35	4.18
LECC90	90%	1290	44	12.80	3.41

Fig. 10 Compressive strength and density with different % of FAC as replacement of sand

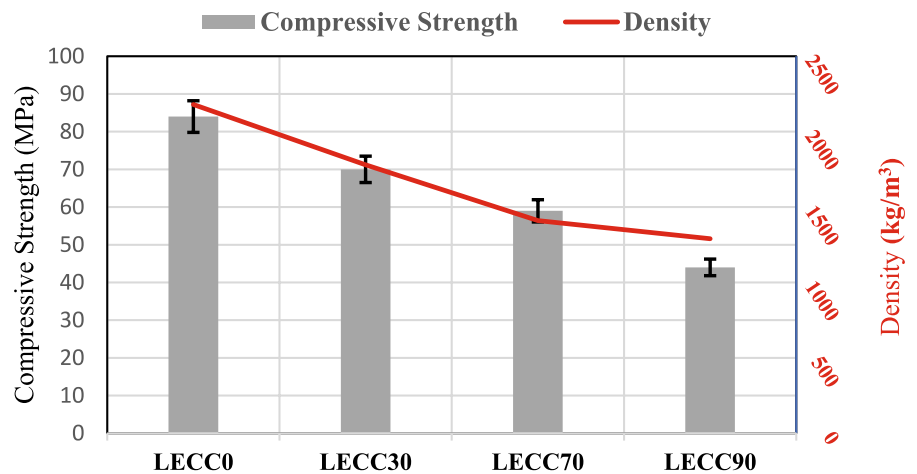
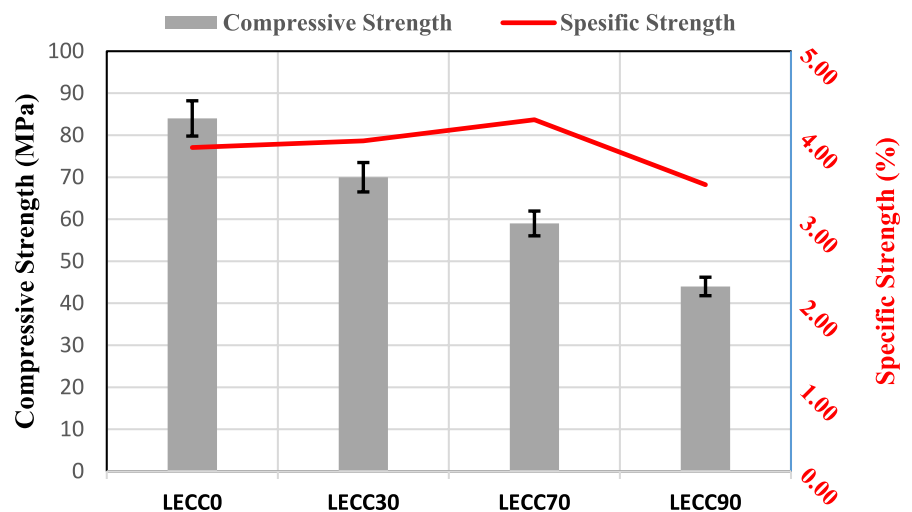


Fig. 11 Compressive strength and specific strength with different % of FAC as replacement of sand



3.2 Slant shear and Bi-surface bond strength test results

Tests for slant shear and bi-surface shear have yielded bond strength values for the composite HLWC substrate—LECC overlay specimens; these values indicate the average bond strengths. Table 14 shows the sample bond strength values.

Based on the outcomes of the slant shear test, the applied stress (σ_0) on the interfacial bond was calculated by applying Eq. (1) to divide the maximum force at bond failure derived from compression loading by the elliptical area (A_e). The bonding shear strength has been determined using the bi-surface shear test by dividing the highest applied force by the bonded surface area, or Eq. (5). Figures 12 and 13 show the average bi-surface and slant shear strengths for HLWC that are 28 days old, with surface preparations of as-cast and grooved surfaces. The slant shear approach produced stronger bond strengths for HLWC substrates than the bi-surface shear method for all LECC repair materials (varying FAC percentages) and surface preparations. This could be

attributed to the fact that the slant shear test's high compressive stresses lead to increased friction forces and interlock, which raise the shear failure load (A [26]). Additionally, it was observed that the maximum bond strengths declined with increasing the FAC content, this could be attributed to the reduced density and the smoother surface of the FAC relative to natural sand that reduced the ability of concrete to distribute loads effectively [33].

Surface roughness has a significant impact on the strength of the bond between HLWC and the repair material (LECC) in both slant shear and bi-surface shear tests. As seen in Figs. 12 and 13, the samples with grooved surface provided better performance relative to as-cast surface. This could be attributed to the fact that the grooved surface provided better interlock between the rough surface of the HLWC and the overlay material as reported by [11, 25]. Bond strengths of specimens with as-cast surfaces containing up to 70% FAC were higher than those reported by [11] and the samples with grooved surfaces have shown comparable performances.

Table 14 Slant shear bond strength, coefficient of friction, and failure modes of specimens for HLWC-LECC

	Encodings	Slant shear strength, σ_o (Mpa)	Average slant shear strength, σ_o	Shear stress, τ_n (Mpa)	Normal stresses σ_n (Mpa)	coefficient of friction, μ	Failure Mode
Grooved	H-LECC0-G	25.21	26.21	22.69	3.49	2.56	B
	H-LECC0-G	26.33					B
	H-LECC0-G	26.82					B
	H-LECC30-G	20.20	21.85	18.92	3.46	2.39	B
	H-LECC30-G	22.51					C
	H-LECC30-G	22.84	B				
	H-LECC70-G	18.15	18.35	15.89	2.57	3.00	B
	H-LECC70-G	19.01					C
	H-LECC70-G	17.89					C
	H-LECC90-G	8.15	8.25	7.14	1.31	2.42	C
	H-LECC90-G	9.03					B
H-LECC90-G	7.57	D					
As-cast	H-LECC0-A	18.88	18.39	15.92	2.42	2.47	B
	H-LECC0-A	19.23					C
	H-LECC0-A	17.06					B
	H-LECC30-A	17.05	16.81	14.55	2.27	1.46	B
	H-LECC30-A	14.78					B
	H-LECC30-A	18.60					C
	H-LECC70-A	13.46	14.64	12.67	1.80	2.17	C
	H-LECC70-A	14.78					C
	H-LECC70-A	15.68					C
	H-LECC90-A	7.85	7.16	6.20	0.96	1.44	B
	H-LECC90-A	7.01					D
H-LECC90-A	6.62	C					

3.3 The coefficient of friction

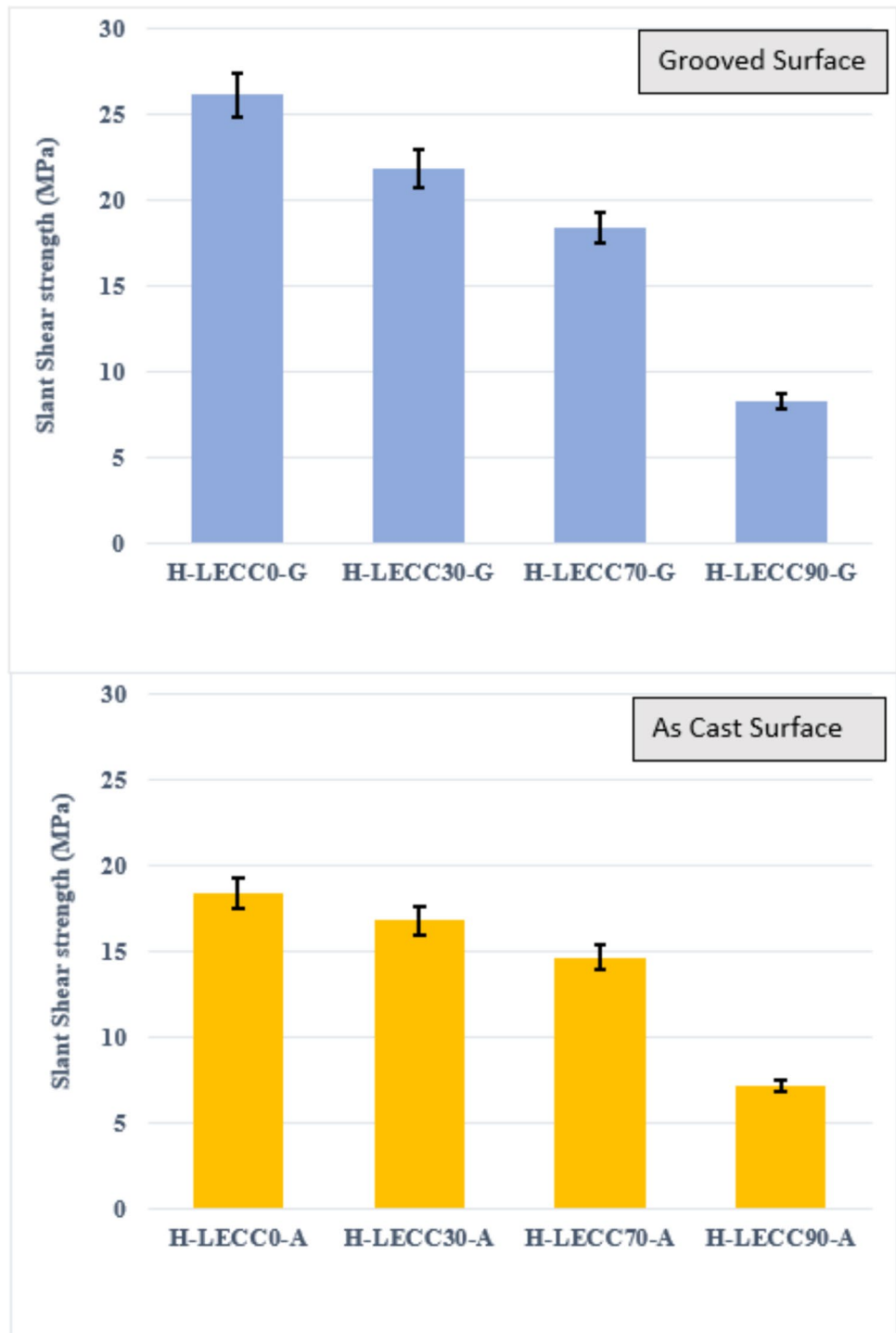
Table 14 summarizes the computed coefficient of friction (μ) values for the specimens under study. The results obtained show that as compared to as-cast specimens, there was an increase in the μ values between the overlay of the grooved surface specimens and the substrate (HLWC). The values of μ ranged from 2.39 to 3.00 and 1.44 to 2.47 for the grooved and as-cast substrate specimens, respectively. The μ results show that the kind of substrate surface preparation and the interlocking effects between the overlay and concrete substrate are responsible for the high μ values of grooved surface relative to as-cast surface [11].

3.4 The failure modes

The location of the failure, which may be represented by several failure modes that are visually inspected and documented, can provide insight into the quality of the connection between the HLWC substrate and the overlay material (LECC). The failure modes were classified into four types, interfacial bond failure -**A**-, interface failure and small pieces

(thin layer) broken on the HLWC substrate -**B**- as shown in Fig. 14. Interfacial failure with a thick layer of HLWC substrate -**C**- as shown in Fig. 15, and complete substrate failure -**D**- as shown in Fig. 16. A significant case of failure modes in the slant shear test and bi-surface shear test occurred across the HLWC substrate, except for a few cracks in the LECC overlay of the as-cast and grooved substrate surface. Moreover, in some cases specifically, in samples with 0–70% FAC interface failure occurred after failure in the HLWC substrate, and there was no separation between the LECC layer and the substrate, indicating the strength of the bonding (26.21–18.35 Mpa, respectively) between those layers. Regarding the composite specimen's complete failure, it occurred in only two cases where the strength of the LECC was comparatively low to the HLWC as shown in Fig. 16. Interfacial failure with a thick layer of HLWC substrate -**C**- was identified as the most favorable failure mechanism. Subsequently, the occurrence of interfacial failure involves the fragmentation of tiny fragments, namely a thin layer, on the HLWC substrate -**B**-. In general, it can be seen that LECC exhibits more strength compared to HLWC, providing a stronger contact in LECC-HLWC composite constructions. The bond strength exhibited excellent

Fig. 12 Average slant shear bond strengths

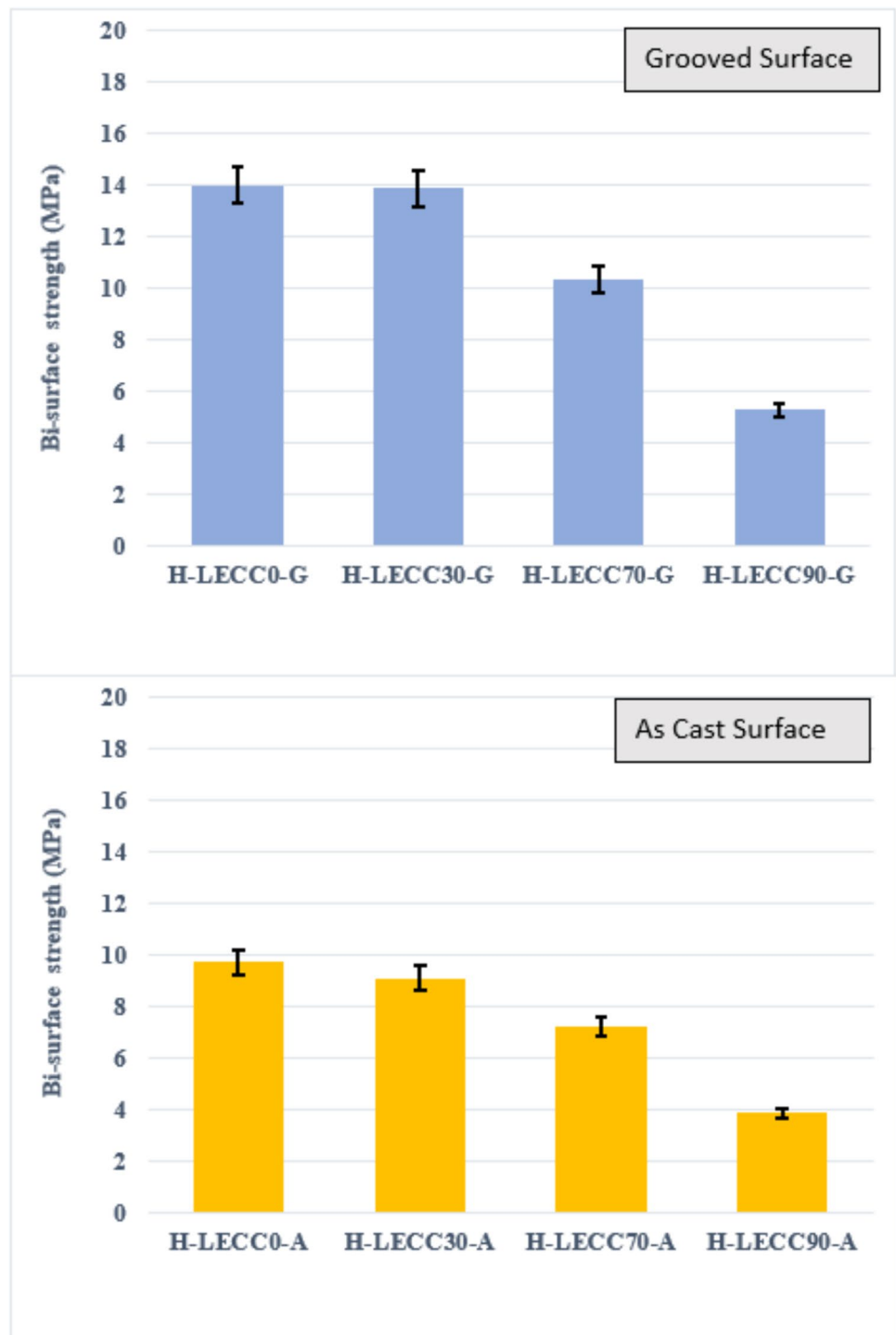


Adhesive force and resilience, as shown by the occurrence of interface failure after the damage of the HLWC substrate.

4 Conclusions

This study investigated the bond behavior at the interface between hybrid fiber-reinforced lightweight ECC containing a high-volume fraction of FAC and high-strength lightweight concrete surfaces with different surface preparations. Based on the findings on this research, the following conclusions were drawn:

Fig. 13 Average Bi-surface strengths



- In the development of LECC, replacing the sand with 70% FAC resulted in a notable decrease in density reached about 35%, and provided a higher specific strength ratio of about (8.6%) relative to the mixture with 0% FAC.
- For the slant shear test, the replacement of sand with 30% FAC in the LECC resulted in a reduction of the bond strength by about 9% and 16% for as-cast surface preparation and grooved surface preparation, respectively relative to the control mixture. This reduction reached about 20% and 30%, respectively when FAC content reached 70%.
- Regarding the bi-surface shear test, results indicated that replacing the sand with 70% FAC in the LECC resulted in a reduction of the bond strength by about 25% for both

Fig. 14 Interface failure and small pieces (thin layer) broken on the HLWC substrate -B-

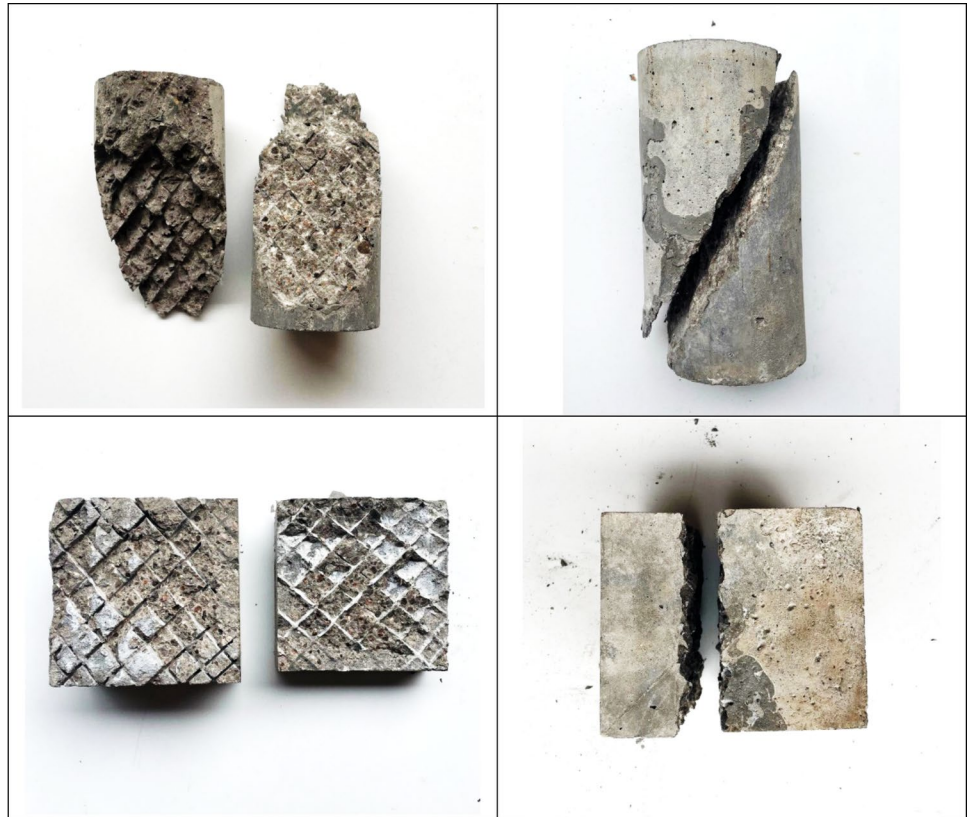


Fig. 15 Interfacial failure with a thick layer of HLWC substrate -C-



Fig. 16 Complete substrate failure -D-



as-cast and grooved surface preparations relative to the control mixtures with 0% FAC.

- The surface grooved treatment increased the coefficient of friction between the repair material (LECC) and HLWC layer.
- The production of an LECC repair material with a high specific strength ratio provides an outstanding strength-to-weight reduction ratio, making it the perfect option for repair applications where load-bearing capability are essential.

Author contributions Haider M. Al-Baghdadi: Conceptualization, Methodology, Investigation. Mohammed M. Kadhum: Supervision, Methodology, Investigation. Ali Shubbar: Writing—Original draft preparation, Methodology.

Funding The authors have not disclosed any funding.

Data availability No datasets were generated or analysed during the current study.

Declarations

Conflict of interest The authors declare no competing interests.

Open Access This article is licensed under a Creative Commons Attribution 4.0 International License, which permits use, sharing, adaptation, distribution and reproduction in any medium or format, as long as you give appropriate credit to the original author(s) and the source, provide a link to the Creative Commons licence, and indicate if changes were made. The images or other third party material in this article are included in the article's Creative Commons licence, unless indicated otherwise in a credit line to the material. If material is not included in the article's Creative Commons licence and your intended use is not permitted by statutory regulation or exceeds the permitted use, you will need to obtain permission directly from the copyright holder. To view a copy of this licence, visit <http://creativecommons.org/licenses/by/4.0/>.

References

1. ACI 211.2-98 (2004) Standard practice for selecting proportions for structural lightweight concrete
2. ACI. 211.4R-08 (2008) Guide for selecting proportions for high-strength concrete using portland cement and other cementitious materials
3. Al-Baghdadi HM, Kadhum MM (2024) Effects of different fiber dosages of PVA and glass fibers on the interfacial properties of lightweight concrete with engineered cementitious composite. *Buildings* 14(8):2379
4. ASTM C39/C39M (2020) Standard test method for compressive strength of cylindrical concrete specimens
5. ASTM C109/C109M-13e1 (2013) Standard test method for compressive strength of hydraulic cement mortars (Using 2-in. or [50-mm] cube specimens). ASTM International. West Conshohocken, PA
6. ASTM C128 (2004) Standard test method for density, relative density (Specific gravity), and absorption of coarse aggregate
7. ASTM C293/C293M (2021) Standard test method for flexural strength of concrete (Using simple beam with center-point loading)
8. ASTM C330 (2017) Standard specification for lightweight aggregates for structural concrete
9. ASTM C642-21 (2022) Standard test method for density, absorption, and voids in hardened concrete
10. ASTM C882/C882M (2020) Standard test method for bond strength of epoxy-resin systems used with concrete by slant shear
11. Behforouz B, Tavakoli D, Gharghani M, Ashour A (2023) Bond strength of the interface between concrete substrate and overlay concrete containing fly ash exposed to high temperature *Structures*, vol 49. Elsevier, pp 183–197
12. Beushausen H, Höhlig B, Talotti M (2017) The influence of substrate moisture preparation on bond strength of concrete overlays and the microstructure of the OTZ. *Cem Concr Res* 92:84–91
13. Brandt A, Olek J, Marshall I (2009) Properties of fiber reinforced cement composites with cenospheres from coal ash. *Brittle Matrix Compos* 9:245
14. BSI (2002) 450-1, Fly ash for concrete-part 1: definitions, specifications and conformity criteria
15. BSI (2011) BS EN 197-1: 2011. Cement, composition specifications and conformity criteria for common cements. British Standard Institution (BSI), London, England

16. Dudziak S, Jackiewicz-Rek W, Kozyra Z (2021) On the calibration of a numerical model for concrete-to-concrete interface. *Materials* 14(23):7204
17. Espeche AD, León J (2011) Estimation of bond strength envelopes for old-to-new concrete interfaces based on a cylinder splitting test. *Constr Build Mater* 25(3):1222–1235
18. Gao S, Zhao X, Qiao J, Guo Y, Hu G (2019) Study on the bonding properties of engineered cementitious composites (ECC) and existing concrete exposed to high temperature. *Constr Build Mater* 196:330–344
19. Hanif A, Lu Z, Diao S, Zeng X, Li Z (2017) Properties investigation of fiber reinforced cement-based composites incorporating cenosphere fillers. *Constr Build Mater* 140:139–149
20. Hanif A, Parthasarathy P, Lu Z, Sun M, Li Z (2017) Fiber-reinforced cementitious composites incorporating glass cenospheres—Mechanical properties and microstructure. *Constr Build Mater* 154:529–538
21. Iraqi Standards NO.5 (1984) Portland cement. Baghdad, Iraq. : The cement agency for standardization and quality control
22. Iraqi Standards NO.45 (1984) Aggregate from natural sources for concrete and building construction. The cement agency for standardization and quality control, Baghdad, Iraq
23. Jin Q, Li VC (2019) Development of lightweight engineered cementitious composite for durability enhancement of tall concrete wind towers. *Cement Concr Compos* 96:87–94
24. Master Builders Solutions (2022) MasterRoc® MS 610. Retrieved from <https://assets.construction-chemicals.mbcc-group.com/en-mne/masterroc-ms-610-tds.pdf>
25. Mirmoghtadaei R, Mohammadi M, Samani NA, Mousavi S (2015) The impact of surface preparation on the bond strength of repaired concrete by metakaolin containing concrete. *Constr Build Mater* 80:76–83
26. Momayez A, Ehsani M, Ramezani pour A, Rajaie H (2005) Comparison of methods for evaluating bond strength between concrete substrate and repair materials. *Cem Concr Res* 35(4):748–757
27. Momayez A, Ramezani pour AA, Rajaie H, Ehsani MR (2004) Bi-surface shear test for evaluating bond between existing and new concrete. *Mater J* 101(2):99–106
28. Omar B, Fattoum K, Maissen B, Farid B (2010) Influence of the roughness and moisture of the substrate surface on the bond between old and new concrete. *Contemporary Eng Sci* 3(3):139–147
29. Pakravan H, Jamshidi M, Latifi M (2018) The effect of hydrophilic (polyvinyl alcohol) fiber content on the flexural behavior of engineered cementitious composites (ECC). *J Textile Inst* 109(1):79–84
30. Patel SK, Satpathy HP, Nayak AN, Mohanty CR (2020) Utilization of fly ash cenosphere for production of sustainable lightweight concrete. *J Inst Eng (India): Series A* 101(1):179–194
31. Ranjith S, Venkatasubramani R, Sreevidya V (2017) Comparative study on durability properties of engineered cementitious composites with polypropylene fiber and glass fiber. *Arch Civil Eng*, 63(4)
32. Sabah SA, Hassan M, Bunnori NM, Johari MM (2019) Bond strength of the interface between normal concrete substrate and GUSMRC repair material overlay. *Constr Build Mater* 216:261–271
33. Satpathy H, Patel S, Nayak A (2019) Development of sustainable lightweight concrete using fly ash cenosphere and sintered fly ash aggregate. *Constr Build Mater* 202:636–655
34. Shang X-y, Yu J-t, Li L-z, Lu Z-d (2019) Strengthening of RC structures by using engineered cementitious composites: a review. *Sustainability* 11(12):3384
35. Singh M, Saini B, Chalak H (2019) Performance and composition analysis of engineered cementitious composite (ECC)—a review. *J Building Eng* 26:100851
36. Singh M, Saini B, Chalak H (2019b) Properties of engineered cementitious composites: a review proceedings of the 1st international conference on sustainable waste management through design: IC_SWMD 2018 1. Springer, Cham, pp. 473–483
37. Singh M, Saini B, Chalak H (2024) Efficacy of hybrid fibre reinforced ECC in RC exterior beam-column connections. *Iranian J Sci Technol, Trans Civil Eng* 48:1–16
38. Sui L, Luo M, Yu K, Xing F, Li P, Zhou Y, Chen C (2018) Effect of engineered cementitious composite on the bond behavior between fiber-reinforced polymer and concrete. *Compos Struct* 184:775–788
39. Tang Z, Litina C, Al-Tabbaa A (2021) Optimisation of rheological parameters and mechanical properties of engineered cementitious composites (ECC) using regression-based models. *Constr Build Mater* 310:125281
40. Wang B, Xu S, Liu F (2016) Evaluation of tensile bonding strength between UHTCC repair materials and concrete substrate. *Constr Build Mater* 112:595–606
41. Wang J-Y, Zhang M-H, Li W, Chia K-S, Liew RJ (2012) Stability of cenospheres in lightweight cement composites in terms of alkali-silica reaction. *Cem Concr Res* 42(5):721–727
42. Wang S, Li VC (2007) Engineered cementitious composites with high-volume fly ash. *ACI Mater J* 104(3):233
43. Wu Y, Wang J-Y, Monteiro PJ, Zhang M-H (2015) Development of ultra-lightweight cement composites with low thermal conductivity and high specific strength for energy efficient buildings. *Constr Build Mater* 87:100–112
44. Xu L-Y, Huang B-T, Dai J-G (2021) Development of engineered cementitious composites (ECC) using artificial fine aggregates. *Constr Build Mater* 305:124742
45. Yu J, Lin J, Zhang Z, Li VC (2015) Mechanical performance of ECC with high-volume fly ash after sub-elevated temperatures. *Constr Build Mater* 99:82–89
46. Yu J, Wu H-L, Leung CK (2020) Feasibility of using ultrahigh-volume limestone-calcined clay blend to develop sustainable medium-strength Engineered Cementitious Composites (ECC). *J Clean Prod* 262:121343
47. Zanjad N, Pawar S, Nayak C (2022) Use of fly ash cenosphere in the construction Industry: a review. *Mater Today: Proc* 62:2185–2190
48. Zanotti C, Rostagno G, Tingley B (2018) Further evidence of interfacial adhesive bond strength enhancement through fiber reinforcement in repairs. *Constr Build Mater* 160:775–785
49. Zhou Y, Xi B, Sui L, Zheng S, Xing F, Li L (2019) Development of high strain-hardening lightweight engineered cementitious composites: design and performance. *Cement Concr Compos* 104:103370
50. Zhu H-G, Leung CK, Cao Q (2011) Preliminary study on the bond properties of the PDCC concrete repair system. *J Mater Civ Eng* 23(9):1360–1364

Publisher's Note Springer Nature remains neutral with regard to jurisdictional claims in published maps and institutional affiliations.